

AIAA 81-0417R

# Shuttle Boundary-Layer Transition Due to Distributed Roughness and Surface Cooling

John J. Bertin\* and Timothy E. Hayden†  
The University of Texas at Austin, Austin, Texas  
and  
Winston D. Goodrich‡  
The Johnson Space Center, Houston, Texas

The transition criteria for the windward surface of the Shuttle Orbiter, which is composed of a large number of thermal protection tiles, must include the effect of distributed roughness arising from joints and possible tile misalignments. Theoretical flowfield parameters and heat-transfer distributions were used to analyze boundary-layer transition data. Data were obtained for Mach numbers from 8 to 12 over a range of Reynolds number based on model length from  $1.8$  to  $17.6 \times 10^6$  with surface temperatures from  $0.114$  to  $0.435 T_t$ . The transition correlations were approximately the same both for the misaligned-tile models and for the grit-roughened model. The incipient value of  $Re_{k,lr}$  was 30, the critical value was 110, and the effective value was 180.

## Nomenclature

$h$	= local heat-transfer coefficient
$h_{t,ref}$	= heat-transfer coefficient for the stagnation point of the reference sphere
$k$	= height of the misaligned tiles
$L$	= axial model length, 0.5734 m (1.881 ft)
$M$	= Mach number
$Re_k$	= Reynolds number based on conditions at the top of the misaligned tile [Eq. (1)]
$Re_y$	= Reynolds number based on the flow conditions at a distance $y$ from the wall
$Re_\theta$	= Reynolds number based on local flow properties and the momentum thickness
$Re_{\infty,L}$	= Reynolds number based on freestream flow properties and the model length
$T$	= temperature
$U$	= streamwise component of the velocity
$x$	= axial coordinate
$\alpha$	= angle of attack
$\delta^*$	= displacement thickness
$\theta$	= momentum thickness
$\mu$	= viscosity
$\xi$	= relative transition location defined in Eq. (2)
$\rho$	= density

## Subscripts

$e$	= evaluated at the edge of the boundary layer
$i$	= evaluated at the particular run of interest [see Eq. (2)]
$t$	= evaluated at the stagnation conditions
$tr$	= evaluated at the transition location
$w$	= evaluated at the wall
$\infty$	= evaluated at the freestream conditions

Presented as Paper 81-0417 at the AIAA 19th Aerospace Sciences Meeting, St. Louis, Mo., Jan. 12-15, 1981; submitted March 11, 1981; revision received March 11, 1982. This paper is declared a work of the U.S. Government and therefore is in the public domain.

\*Bettie Margaret Smith Professor of Engineering, Department of Aerospace Engineering and Engineering Mechanics. Associate Fellow AIAA.

†Research Assistant, Department of Aerospace Engineering and Engineering Mechanics. Member AIAA.

‡Aerospace Technologist, Aerothermodynamics Section. Associate Fellow AIAA.

## Introduction

IN order to predict the convective heat-transfer distribution for the windward surface of the Space Shuttle entry configuration, one must develop engineering correlations for the three-dimensional, compressible boundary layer. Since the aerodynamic heating rates generated by a turbulent boundary layer may be several times greater than those for a laminar boundary layer at the same flight condition, the correlations must include a transition criteria suitable for the complex flowfields. Because the windward surface of the Orbiter is composed of a large number of thermal protection tiles, the transition criteria must include the effect of the distributed roughness arising from joints and tile misalignments.

Dryden<sup>1</sup> noted that "the roughness element imposes a disturbance that is added to those already present in the initial turbulence of the stream. Its contribution to the total disturbance within the critical wavelength range for which amplification occurs depends on its shape and its height relative to the ratio of the height of the cylindrical roughness element (wire) to the boundary-layer displacement thickness ( $k/\delta^*$ ) for low-speed flow past a flat plate." It was noted, however, that "the height of the roughness element was never increased sufficiently to bring transition forward to the element" for these tests.

Klebanoff et al.<sup>2</sup> presented low-speed data where the transition measurements downstream of two-dimensional roughness elements exhibited a relationship between  $Re_{k,lr}$  and  $k/\delta^*$  consistent with Dryden's findings, whereas those for three-dimensional (spherical) roughness elements did not. For spherical roughness elements (where diameter and spacing were test parameters), Klebanoff et al. presented  $Re_{x,tr}$  as a function of  $Re_k$ . The roughness was essentially without effect until a critical value of  $Re_k$  was reached, beyond which transition rapidly moved forward toward the trips. The "average" critical value of  $Re_k$  was 577 for spherical elements and was between 200 and 300 for two-dimensional roughness elements.

In a study of transition induced by spherical roughness elements on a cone where the local Mach number was 2.71, van Driest and Blumer<sup>3</sup> discussed the concept of "effective tripping." At relatively low (unit) Reynolds numbers, freestream disturbances dominated and the roughness-promoted transition location was only slightly upstream of that for a smooth model. At some point, "the roughness element has become large enough relative to the boundary-

layer thickness to produce a drastic forward movement of transition." At higher unit Reynolds numbers, the roughness elements were predominant in establishing transition, and transition occurred just downstream of the roughness elements. A trip was defined as effective when the Reynolds number of transition at this location was a minimum.

When a narrow strip of sand-grain/distributed-roughness elements was used as the tripping device on a flat plate in low-speed flows,<sup>4</sup> the value of  $Re_k$  to just affect boundary-layer transition was found to be in the 250-300 range, while values of approximately 400 were required to bring transition to the trip location itself.

Reviewing low-speed measurements which covered a wide range of particle shape, distribution, number, height, distance from the model leading edge, and degree of boundary-layer stability, Braslow<sup>5</sup> noted that "In spite of large differences in roughness configuration and differences in experimental technique, the values of  $\sqrt{Re_{k,tr}}$  for transition for a given value of  $d/k$  (width/height) are seen to vary only within a factor of about 2." Furthermore, Braslow noted that this same range of critical roughness Reynolds numbers was found to exist up to Mach numbers of about 4.

McCauley et al.<sup>6</sup> observed that, if the spherical elements were spaced too closely together, the trips became less effective in promoting transition. Braslow<sup>7</sup> cited measurements which indicated that for close streamwise spacing, the critical roughness height increased somewhat, because the presence of a rearward particle tended to delay the formation of eddies around the first particle. Thus the tripping effectiveness is a function not only of the roughness elements heights and shapes but of their spacing (and the extent of surface covered).

Rough-wall transition criteria were developed using data from hypersonic wind tunnel tests utilizing roughened, nonporous, thin-walled models.<sup>8</sup> A relative roughness parameter  $(T_e/T_w)(k/\theta)$  was identified as the disturbance parameter which correlates with the momentum thickness Reynolds number at transition. Ballistic range data presented by Reda<sup>9</sup> indicated that  $Re_{k,tr} \approx 100$  for the case of three-dimensional roughness elements distributed spatially over the entire surface of a preablated nosetip. Reda concluded, however, that the parameter

$$[\rho_k U_k k / \mu_w]_{tr} = \text{const}$$

best represents the physics of roughness-dominated transition on blunt bodies in hypersonic flows. If the curvature correction term is not applied,  $(\rho_k U_k k / \mu_w)_{tr} \approx 200$ .

The effect of tile misalignment and surface temperature on boundary-layer transition in the windward pitch plane of the Shuttle Orbiter has been studied by Bertin, Idar, and Goodrich.<sup>10</sup> The correlations were based on heat-transfer data obtained in Tunnel B (AEDC) for surface temperatures from 0.12 to 0.42  $T_i$  with surface-roughness elements simulating vertically misaligned heat-shield tiles. The ratio of the roughness-promoted transition location to the smooth-body location was correlated in terms of the ratio  $(\delta^*/k)$  evaluated at  $x \approx 0.1L$ . Although real-gas solutions for the Shuttle Orbiter boundary layer produced only positive values of  $\delta^*$  (Ref. 11),  $\delta^*$  can be negative for accelerated flows past highly cooled walls. Thus, it may be desirable to develop transition correlations using parameters other than the displacement thickness. Furthermore, the literature cited above indicate that a parameter such as  $Re_k$  may be more appropriate for three-dimensional distributed roughnesses.

Since the transition correlations developed thus far do not include a measure of the roughness-element spacing (or periodicity of the flow perturbations), the data base was extended to include Orbiter transition "measurements" for a grit-roughened model. Thus, alternative correlations are developed in the present paper using both the data of Ref. 10 and previously unreported data.

## Experimental Program

A primary objective of the present investigation was to determine what effect tile misalignment representative of a reasonable manufacturing tolerance has on the heat-transfer distribution in the plane of symmetry of the Shuttle Orbiter. To do this, the heat-transfer data from test programs conducted in Tunnel B and in Tunnel F of the AEDC were studied. The data were obtained over a range of freestream Mach number from 8 to 12 over a range of freestream Reynolds numbers (based on model length) from 1.8 to  $17.9 \times 10^6$ . The stagnation temperature ranged from 700 to 1570 K. The surface temperature was varied from 0.114 to 0.435  $T_i$ . The data presented in the present paper were obtained at an angle of attack of 30 deg.

## Models

The basic model used in the test programs was a 0.0175-scale model of the Space Shuttle configuration defined by Rockwell drawing VL70-000139 and designated model 29-0 (see Ref. 12). Twenty-seven coaxial surface thermocouples were used to obtain the heat-transfer-rate distribution for the windward plane of symmetry.

To study the effect of tile misalignment, selected tiles were etched (or deposited depending on the misalignment height) on the windward surface, so that they were slightly above the model surface. The misaligned tiles formed a herringbone pattern (symmetric about the plane of symmetry) covering the windward surface of the Orbiter model up to the tangent line of the chines from  $x=0.02$  to  $0.80L$ . The raised tiles, which were selected randomly, represented 25% of the tiles in the area of interest, as shown in the photograph of Fig. 1. The selected tiles were 0.267 cm (0.105 in.) square. The character of the model surface for each of the Tunnel B test programs is summarized below.

### OH4A Test Program

For the OH4A tests, the surface of the 0.0175-scale Orbiter model was smooth. Thus the transition locations determined from the heat-transfer distributions serve as the reference, or smooth-body, transition locations. The reader is referred to Ref. 13 for the basic data and for additional information regarding these tests.

### MH2A Test Program

For the MH2A tests, the misaligned tiles were deposited to a height of approximately 0.0025 cm (0.0010 in.). The vertical misalignment, thus simulated, was 0.1451 cm (0.0571 in.) full-scale. Thus, the nondimensionalized tile height  $(k/L)$  for this model was  $4.43 \times 10^{-5}$ . The basic data for this tile misalignment height (designated  $k_1$  in the present report) are presented in Ref. 14.

### MH2B Test Program

For the MH2B tests, the surface surrounding the tiles was removed until the misaligned tiles were approximately 0.0051 cm (0.0020 in.) in height. This misalignment, which is

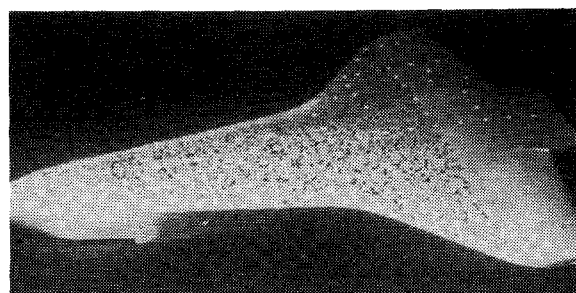


Fig. 1 Photograph of the model (used in the Tunnel B tests) showing randomly misaligned tiles.

designated  $k_2$  in the present report, corresponds to a full-scale vertical misalignment of 0.2903 cm (0.1143 in.). For the  $k_2$  misalignment,  $k$  was  $8.86 \times 10^{-5} L$ . Additional information about the model and the basic data for the MH2B program are presented in Ref. 15.

#### Tunnel F Test Program

Heat-transfer distributions were obtained on a similar model in Tunnel F at AEDC.<sup>16,17</sup> For the Tunnel F tests, 80% of the windward surface was roughened using a grit-blasting technique. The average peak-to-valley distance for ten readings in a 0.25 cm length (as read from a photomicrograph) was 0.0041 cm. For this model,  $k$  was  $7.09 \times 10^{-5} L$ . Since the flow conditions of Tunnel F vary during the course of a run, several test conditions can be obtained during a single run. Thus, although data will be presented for only three runs, 16 flow conditions are represented.

### Discussion of Results

The effects of the height of the misaligned tiles and the surface temperature on the heat-transfer distribution for the plane of symmetry when the Orbiter is at an angle of attack of 30 deg are illustrated in the data presented in Fig. 2. Data are presented from tests where the freestream Mach number was 8.0, the freestream Reynolds number based on the model length was  $7.1 \times 10^6$ , and the surface temperature was either 300 K ( $0.40 T_f$ ) or in the range 96-127 K ( $0.128-0.171 T_f$ ). The heat-transfer distributions are presented as the dimensionless ratio  $h/h_{t,ref}$ , which involves the experimental value of the local heat-transfer rate divided by the theoretical heat-transfer rate to the stagnation point of a 0.00533-m (0.0175-ft) radius sphere, as calculated using the theory of Fay and Riddell.<sup>18</sup> For purposes of data presentation, the recovery factor has been set equal to unity.

Heat-transfer distributions for theoretical solutions of a nonsimilar laminar boundary layer using the small cross-flow axisymmetric analog to represent the three-dimensional character of the boundary layer, which were calculated using

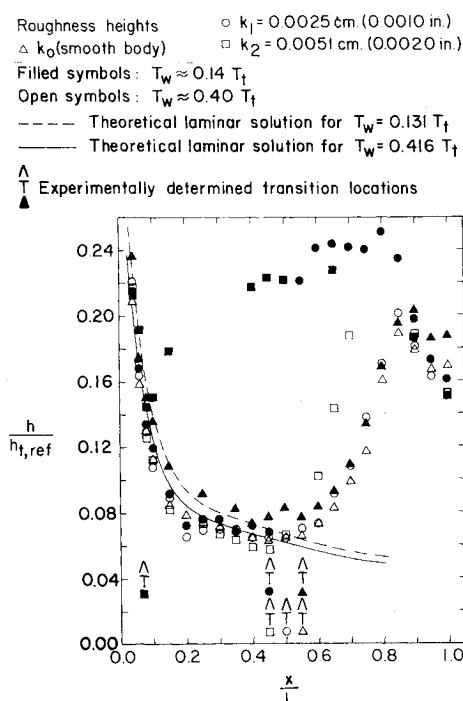


Fig. 2 Effect of tile-misalignment height and surface temperature on the heat-transfer distribution for the plane of symmetry;  $\alpha = 30$  deg,  $M_\infty = 8$ ,  $Re_{\infty,L} = 7.1 \times 10^6$ .

the numerical code of Ref. 19, are included in Fig. 2. Required as input for the boundary-layer code were the static pressures, the entropy at the edge of the boundary layer, and the radius of the "equivalent" body of revolution. Because the bow shock wave is curved, the entropy varies throughout the shock layer. Thus, the local flow properties at the edge of the boundary layer were evaluated using the entropy and the surface pressure distributions calculated using the numerical code of Ref. 20.

Theoretical Mach number profiles indicated<sup>21</sup> that the misaligned tiles would protrude into the sonic regions of an unperturbed laminar boundary layer over much of the body. Thus, one would expect that the presence of the misaligned tiles would significantly perturb the flowfield. This is verified in the shadowgraphs,<sup>10</sup> where easily visible waves emanate from the tiles. A highly vortical flow results when the turbulent boundary layer flows over the misaligned tiles. Nevertheless, as can be seen in the data of Fig. 2, tile misalignment did not significantly affect the heat-transfer rates, where the boundary layer was either laminar or turbulent for the conditions of these wind tunnel tests. The heating distributions calculated using this variable entropy flow model are in good agreement with the laminar data. Theoretical values for the nondimensionalized heat-transfer coefficient were slightly greater for the colder surface, i.e.,  $T_w = 0.131 T_f$ . The increased heating is attributed to the increased velocity gradients and viscous dissipation, which result when the boundary-layer thickness is decreased by surface cooling, i.e., as  $T_w/T_f$  decreases. The data presented in Fig. 2 are consistent with the theoretically determined effect of surface temperature. However, if one reviews all of the data from these tests,<sup>21</sup> there is no clear correlation between the experimental values of the nondimensionalized local heating and the surface temperature. This lack of correlation is of little significance, since the theoretical solutions predict less than a 15% change in heat-transfer level, and the experiment was not designed to resolve changes of this magnitude.

The heat-transfer distributions were used to determine the "point" at which boundary-layer transition occurred in the plane of symmetry. The experimentally determined transition location was that point at which the heat transfer deviated from the laminar distribution. The transition locations, thus determined for these representative flow conditions, are presented in Fig. 2. At the higher surface temperature, the misaligned tiles moved transition only slightly upstream relative to the smooth-body transition location (refer to the open symbols in Fig. 2). However, at the lower temperature, tiles which were misaligned 0.0025 cm ( $k_1$ ) moved transition forward by  $0.1L$ , and increasing the tile misalignment height to 0.0051 cm ( $k_2$ ) moved transition well forward. For lower surface temperature and for greater tile misalignment, transition occurred very near the nose, approaching a minimum transition length. The tile-induced boundary-layer perturbation appears to be a function of the height of the tile relative to the displacement thickness. Correlations of the transition location for the Tunnel B data have been presented previously<sup>10</sup> in terms of the displacement thickness including the interdependence between the local Mach number, Reynolds number, surface temperature, and tile misalignment height. The values of this correlation parameter are included in Table 1 for all the test conditions (i.e., those of Tunnel F as well as those of Tunnel B) discussed in the present report.

The effect of surface roughness and of surface temperature on the transition-correlation parameter used in the Shuttle Orbiter design, i.e.,  $Re_\theta/M_e$ , is illustrated by the data presented in Fig. 3. Data are presented for models with herringbone patterns of vertically misaligned tiles which were tested in Tunnel B and for grit-roughened models which were tested in Tunnel F in Figs. 3a and 3b, respectively. Included in this figure are the following parameters.

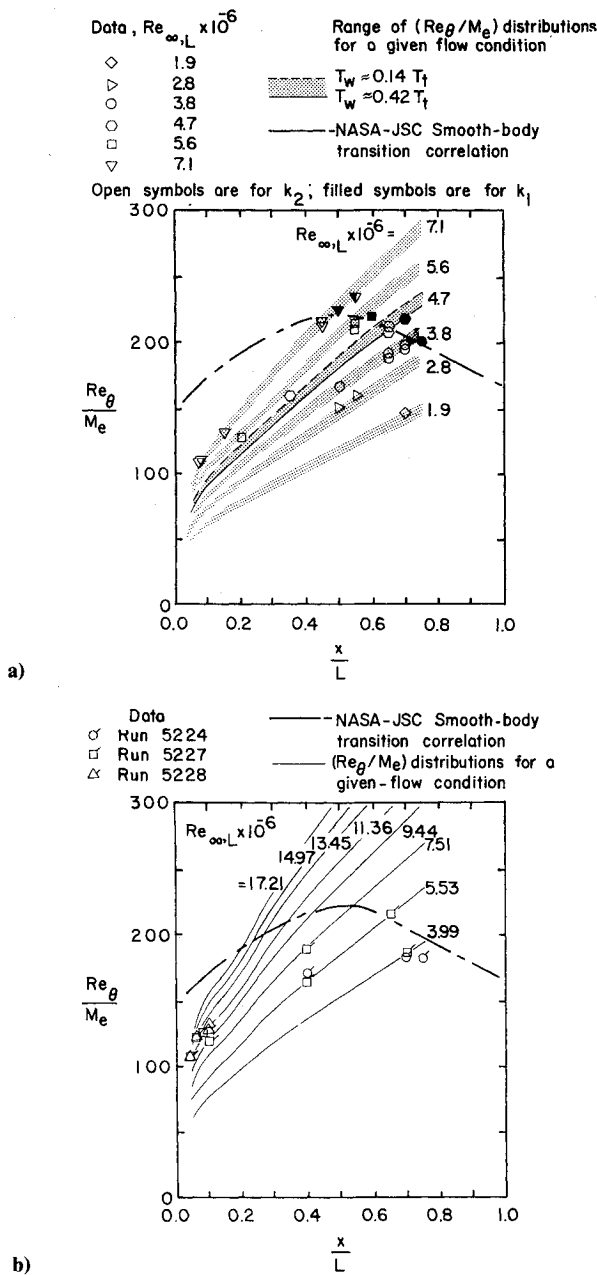


Fig. 3 Streamwise distribution of the Shuttle transition parameter. a) Misaligned-tile model (Tunnel B); b) Grit-roughened model (Tunnel F).

1) The streamwise distributions of the computed values of the parameter  $(Re_{\theta}/M_e)$  for various flow conditions are represented by the shaded region for the Tunnel B conditions and by the solid lines for the Tunnel F tests. Referring to the  $(Re_{\theta}/M_e)$  distributions for  $Re_{\infty,L} = 4.7 \times 10^6$ , the reader can see that the upper bound of the shaded region corresponds to the coldest wall temperature tested, while the lower bound corresponds to the warmest. The relatively large variations in surface temperature have only a small effect on the computed values of  $(Re_{\theta}/M_e)$  at a given location for a given freestream flow.

2) The smooth-body correlation for transition in the Orbiter pitch-plane as developed by the Johnson Space Center (NASA-JSC) is represented by the broken-line fairing.

3) Experimentally determined values of  $(Re_{\theta}/M_e)_{tr}$ , i.e., evaluated at the transition location, are represented by individual symbols. The same relation between a given symbol and the flow condition it represents is maintained in all but Figs. 5 and 7.

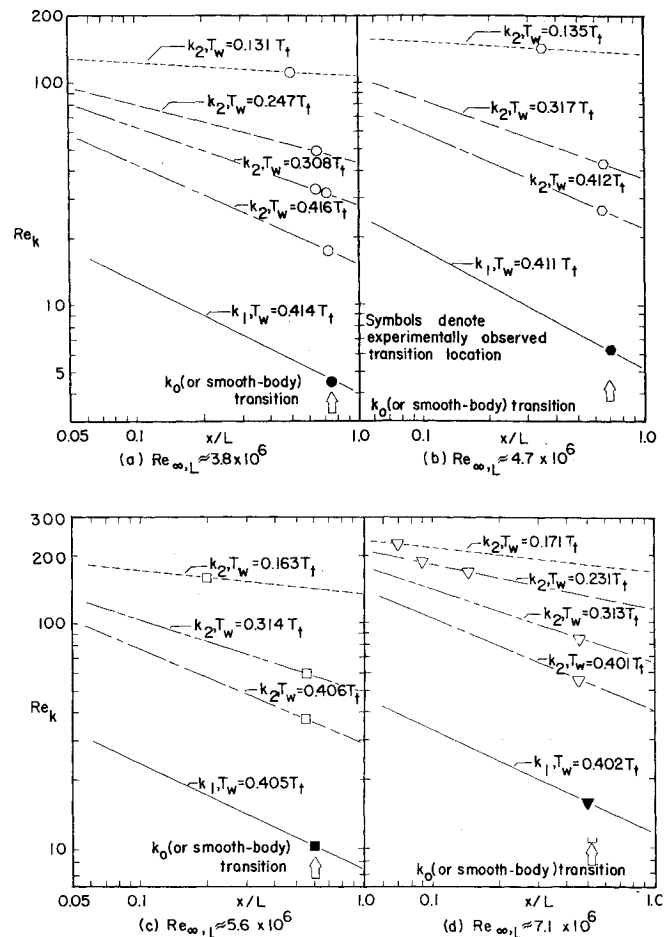


Fig. 4 Streamwise distributions of  $Re_k$  for the Tunnel B tests.

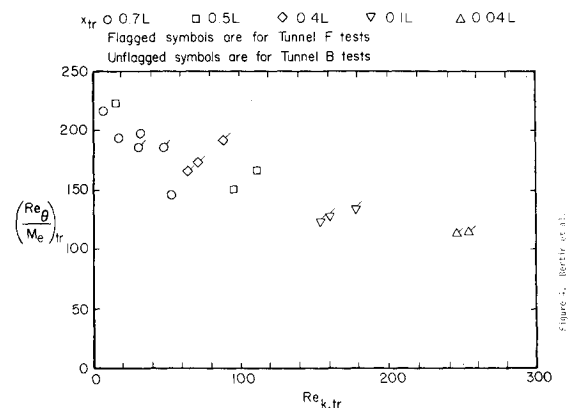


Fig. 5 The Shuttle transition parameter as a function of  $Re_{k,tr}$ .

Note that for parts 2 and 3 the parameters are evaluated at the transition location. Thus, the ordinate is  $(Re_{\theta}/M_e)_{tr}$  and the abscissa is  $x_{tr}/L$ .

The transition locations obtained during Tunnel B tests for the smooth model ( $k_0$ ) are represented by the half-filled symbol and by the filled symbols (when the transition location was the same for the  $k_0$  and  $k_1$  roughness) of Fig. 3a. Note that they follow the smooth-body correlation used by NASA-JSC. The transition locations for the  $k_1$  tiles, i.e., those for which  $k=0.0025$  cm, also are represented by the filled symbols. As noted when discussing the heat-transfer distributions presented in Fig. 2, the  $k_1$  tiles had only a slight effect on the transition location. The greater misalignment of the  $k_2$  tiles coupled with a thinner boundary layer due to

Table 1 Correlation parameters for boundary-layer transition in the windward pitch plane of the Shuttle Orbiter,  $\alpha = 30$  deg

$M_\infty$	$Re_{\infty,L} \times 10^{-6}$	$k/L, \times 10^5$	$T_w/T_t$	$x_{tr}/L$	$(Re_\theta/M_e)_{tr}$	$\xi, \text{Eq. (2)}$	$Re_{x,tr} \times 10^{-5}$	$Re_{k,tr}$	$(Re_k)_{x=0.1L}$	$(\delta^*/k)_{x=0.1L}$
Tunnel B, simulated-tile misalignment										
7.94	1.970	0.00	0.435	w.l. <sup>a</sup>	a	a	a	d	d	d
7.97	2.871	0.00	0.417	0.95	c	b	c	d	d	d
7.98	3.655	0.00	0.411	0.75	200	b	12.12	d	d	d
7.98	4.666	0.00	0.412	0.70	216	b	14.02	d	d	d
7.99	5.619	0.00	0.405	0.60	218	b	13.99	d	d	d
8.00	7.004	0.00	0.400	0.50-0.55	223-234	b	13.83	d	d	d
7.94	1.887	4.43	0.423	w.l. <sup>a</sup>	a	a	a	a	a	a
7.97	2.829	4.43	0.416	0.95	c	c	c	c	c	3.60
7.98	3.652	4.43	0.414	0.75	200	1.000	12.12	4.56	13.03	3.17
7.98	4.632	4.43	0.411	0.70	216	1.000	14.02	6.89	17.93	2.80
7.99	5.625	4.43	0.405	0.60	218	1.000	13.99	10.23	24.18	2.50
8.00	7.064	4.43	0.402	0.50	223	1.000-0.953	13.83	15.62	33.15	2.21
7.94	1.894	8.86	0.423	w.l. <sup>a</sup>	a	a	a	a	a	a
7.97	2.846	8.86	0.418	0.85	c	c	c	c	29.73	1.82
7.98	3.701	8.86	0.416	0.70	193	0.965	11.17	17.76	43.16	1.59
7.98	4.673	8.86	0.412	0.65	206	0.954	12.84	26.18	59.62	1.40
7.99	5.631	8.86	0.406	0.55	208	0.954	12.49	37.36	77.46	1.25
8.00	7.040	8.86	0.401	0.45	211	0.946-0.902	12.03	56.34	105.71	1.10
7.94	1.889	8.86	0.340	w.l. <sup>a</sup>	a	a	a	a	a	a
7.97	2.820	8.86	0.324	0.90	c	c	c	c	42.55	1.33
7.98	3.653	8.86	0.308	0.65-0.70	186-197	0.985-0.930	10.02-11.03	31.64-32.48	63.33	1.09
7.98	4.668	8.86	0.317	0.65	211	0.977	12.80	42.65	82.97	1.00
7.99	5.653	8.86	0.314	0.55	213	0.977	12.51	58.10	103.56	0.90
8.00	7.066	8.86	0.313	0.45	216	0.969-0.923	12.04	85.75	140.21	0.80
7.98	3.661	8.86	0.247	0.65	191	0.955	10.03	48.81	80.53	0.80
8.00	7.077	8.86	0.231	0.08-0.15	111-130	0.583-0.474	1.515-3.136	189-166	181.31	0.51
7.94	1.868	8.86	0.128	0.70	145	e	5.635	52.91	62.78	0.23
7.97	2.835	8.86	0.114	0.50-0.55	149-157	c	5.540-6.273	95.28-95.92	100.46	0.10
7.98	3.661	8.86	0.131	0.50	166	0.830	7.145	110.93	123.17	0.18
7.98	4.637	8.86	0.135	0.35	159	0.736	5.738	141.84	154.08	0.18
7.99	5.616	8.86	0.163	0.20	127	0.583	3.504	159.81	172.62	0.29
8.00	7.072	8.86	0.171	0.07	110	0.493-0.470	1.297	222.1	214.47	0.29
Tunnel F, grit-blasted roughness										
11.76	7.82	7.09	0.249	0.40	172	0.814 <sup>f</sup>	6.102	71.33	117.39	1.10
11.74	5.61	7.09	0.219	0.70	186	0.944 <sup>f</sup>	20.02	47.65	95.24	1.08
11.75	4.65	7.09	0.205	0.75	185	0.969 <sup>f</sup>	18.86	42.09	83.72	1.11
10.80	17.21	7.09	0.283	0.02	c	c	c	c	236.54	0.78
10.79	14.97	7.09	0.266	0.04	113	0.551 <sup>f</sup>	1.172	246.36	216.71	0.78
10.83	13.45	7.09	0.256	0.06	125	0.625 <sup>f</sup>	1.726	225.27	198.46	0.79
10.85	11.36	7.09	0.231	0.08	125	0.598 <sup>f</sup>	2.106	182.19	172.48	0.80
10.78	9.44	7.09	0.227	0.10	122	0.572 <sup>f</sup>	2.380	154.16	154.26	0.80
10.82	7.51	7.09	0.219	0.40	191	0.868 <sup>f</sup>	10.77	87.65	122.44	0.87
10.73	5.53	7.09	0.212	0.40-0.65	166-203	0.788-1.000 <sup>f</sup>	8.139-15.72	63.20-59.24	76.02	0.97
10.83	3.99	7.09	0.224	0.70	186	0.944 <sup>f</sup>	11.86	31.17	54.37	1.24
11.07	17.62	7.09	0.268	0.02	c	c	c	c	249.61	0.74
11.00	15.10	7.09	0.252	0.04	114	0.556 <sup>f</sup>	1.182	254	224.84	0.74
11.04	13.19	7.09	0.249	0.06	122	0.604 <sup>f</sup>	1.662	219	193.41	0.78
11.05	12.45	7.09	0.251	0.10	133	0.633 <sup>f</sup>	2.878	178	177.91	0.82
11.13	12.19	7.09	0.266	0.10	127	0.596 <sup>f</sup>	2.760	160	160.39	0.91

<sup>a</sup> Boundary layer is wholly laminar (w.l.).<sup>b</sup> Since these are the smooth-body transition locations, there can be no  $\xi$ .<sup>c</sup> Flowfield solution was not obtained for this point.<sup>d</sup> Since these are smooth-body solutions,  $k = 0$ .<sup>e</sup> There is no reference value (denominator) for this condition.<sup>f</sup> These are approximate values of  $\xi$  (see text).

cooling moves transition upstream towards the stagnation point, as indicated by the open symbols of Fig. 3a.

No smooth-body data from Tunnel F were obtained during the tests discussed in the present paper. Nevertheless, for four flow conditions, transition for the grit-roughened model occurs near the smooth-body correlation. Thus, the grit-roughened surface causes transition to move upstream by 10%, or less, for these conditions. However, at the highest freestream Reynolds numbers, transition occurs very near the nose.

Because surface roughness causes the transition location to move upstream dramatically at the lower surface temperatures, the values of  $(Re_\theta/M_e)_{tr}$ , i.e., those at the ex-

perimentally determined transition locations, vary significantly, as indicated by the data presented in Fig. 3. Although the data presented in Fig. 3 clearly indicate the effects of surface roughness and of cooling, the parameter  $k$  does not appear (either explicitly or implicitly). As noted in the Introduction, many investigators have used  $Re_k$  to correlate the effects of roughness for three-dimensional roughness elements. Although the ratio of the width to the height ( $k$ ) of the vertically misaligned tiles is either 52.5 or 105, they are not two-dimensional obstacles (recall the comment about the herringbone pattern).

Using the computed solutions for a nonsimilar, laminar boundary layer (as described earlier), the streamwise

distributions of  $Re_k$  were calculated where

$$Re_k = \rho_k U_k k / \mu_k \quad (1)$$

The theoretical  $Re_k$  distributions for the various wall-temperature/tile-misalignment conditions are presented for four different Reynolds numbers for the Tunnel B tests in Fig. 4. Note that the only parameters to change in a given figure are the tile-misalignment height and the surface temperature. Near the nose, where the boundary layer is thin, the velocity and the density at the top of the tile are much larger than the corresponding values at a downstream location. Thus  $Re_k$  decreases in the streamwise direction. The streamwise variation in  $Re_k$  decreases as the surface temperature decreases.

The experimentally determined transition locations are included in Fig. 4. The arrows indicate the smooth-body transition locations: the filled symbols, those for the  $k_1$  configuration, and the open symbols, those for the  $k_2$  configuration. Thus the reader can easily see the effect of tile roughness height and of surface temperature on the value of  $Re_k$  at the transition location, i.e.,  $Re_{k,tr}$ . Note that the value of  $Re_{k,tr}$  is well below the values near the nose, where the boundary layer remains laminar although it has passed over misaligned tiles. Transition moves rapidly toward the nose once a critical value of  $Re_{k,tr}$  is exceeded.

For the low-Reynolds-number flow over the uncooled surface ( $T_w = 0.414T_i$ ) with the  $k_1$ -tile misalignment ( $k = 0.0025$  cm),  $Re_k$  at the experimentally observed transition location is only 4.56, as shown in Fig. 4a. Recall, however, that the transition location for this run is the same as that for the smooth model. For flow over the coldest surface ( $T_w = 0.131T_i$ ) with the  $k_2$ -tile misalignment ( $k = 0.0051$  cm),  $Re_{k,tr} = 110.93$ . For this flow, the tiles do promote transition, since  $x_{tr}$  is  $0.50L$ , whereas transition occurs at  $0.75L$  for flow over the uncooled smooth body at the same freestream conditions. For the highest-Reynolds-number flow,  $Re_{k,tr}$  varies from 15.62 (for which the transition location is essentially the same as that for the smooth body) to 222.11 (for which transition has moved significantly upstream).

Since  $(Re_\theta/M_e)_{tr}$  is the correlation parameter used in the Shuttle design, its relation with  $Re_{k,tr}$  should also be considered. The values of  $(Re_\theta/M_e)_{tr}$  at the experimentally determined transition locations are grouped in Fig. 5 according to the axial station at which transition occurred, i.e.,  $x_{tr}/L$ . As  $Re_{k,tr}$  increases,  $(Re_\theta/M_e)_{tr}$  decreases. It is interesting to note that the correlation of these transition parameters is essentially the same for the grit-roughened model and for the misaligned-tile models.

The correlation of Fig. 5 used the Reynolds number based on the flow properties at the top of the roughness element evaluated at the transition location, i.e.,  $Re_{k,tr}$ . Because

transition occurs at various axial stations, the designer must generate boundary-layer solutions along the entire length of the fuselage at several times during the trajectory. Producing the necessary information, although a formidable task, is made less difficult because  $Re_k$  is relatively insensitive to  $x/L$  at flight conditions. A similar insensitivity occurred for wind-tunnel flows over highly cooled models, as was noted when discussing Fig. 4. However, to simplify the process of extrapolating the wind-tunnel-based correlations for roughness-induced transition to flight conditions, consideration will now be given to correlations using the roughness Reynolds number evaluated at a common axial location for all test conditions. The  $x = 0.1L$  station is chosen because accurate boundary-layer profiles can be obtained at this station and the roughness Reynolds number is near its maximum value at this station.

The axial station at which transition occurs for the grit-roughened model is presented as a function of  $Re_{k,x=0.1L}$  in Fig. 6. There are several points for each of the three runs, since Tunnel F operates as a blowdown tunnel. At relatively low values for the roughness Reynolds number ( $Re_{k,x=0.1L}$ ), the transition location is essentially unaffected by the grit-roughened surface. At intermediate Reynolds numbers, transition moves rapidly upstream toward the nose. For roughness Reynolds numbers at  $x = 0.1L$  in excess of 150, the roughness elements are large relative to the boundary layer and serve as effective tripping elements. This "effective" value of 150 for the roughness Reynolds number is less than that for the Tunnel B measurements (180). Possible reasons for this difference include 1) differences between the character of the roughness elements, and 2) the operational characteristics of Tunnel F. It should be noted that the operation of Tunnel F is such that the Reynolds number decreases with time during a run. Since the maximum Reynolds number occurs at the outset of a run, transition is initially at its most upstream location for that run. Thus it is possible that, since the turbulent boundary layer is already established, it can exist at a lower Reynolds number (as the Reynolds number decreases) than would be required to effectively trip a laminar boundary layer.

The transition parameter,  $(Re_\theta/M_e)_{tr}$ , is presented as a function of  $Re_{k,x=0.1L}$  in Fig. 7. The correlation using the roughness Reynolds number evaluated at  $x = 0.1L$  is qualitatively similar to that which uses the roughness Reynolds number evaluated at the transition location, as was presented in Fig. 5.

Various parameters can be used to quantify the forward movement of transition due to the combined effect of roughening the surface and cooling the wall for a given flow. For this article, the relative transition locations are presented as the ratio  $\xi$ , where

$$\xi = \frac{(Re_\theta/M_e)_{tr,R}}{(Re_\theta/M_e)_{tr,S}} = \frac{[(Re_\theta/M_e)_{tr}] k_i T_{wi} Re_{\infty,L}}{[(Re_\theta/M_e)_{tr}] k_0 0.42 T_i Re_{\infty,L}} \quad (2)$$

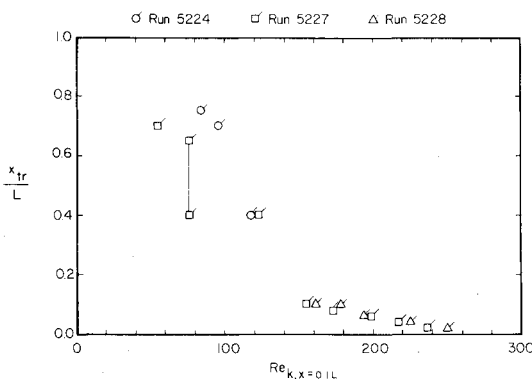


Fig. 6 The transition locations as a function of  $Re_{k,x=0.1L}$  for the grit-roughened model.

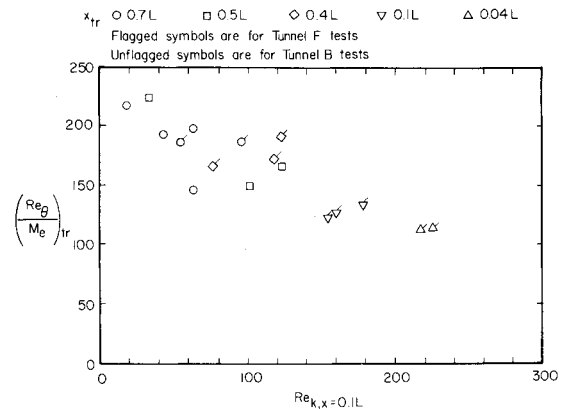


Fig. 7 The Shuttle transition parameter as a function of  $Re_{k,x=0.1L}$ .

Since the reference (or smooth-body) transition location is independent of the wall temperature for the flow conditions of the present study,  $0.42T_i$  merely serves as a reference value.

Experimental values of  $\xi$ , both for the misaligned tiles and for the grit-roughened model, are presented in Fig. 8. These nondimensionalized, relative transition locations represent the ratio of the experimentally determined value of  $(Re_\theta/M_e)_{tr}$  for the surface roughness of a particular run ( $k_i$ ), at the surface temperature of that run ( $T_{wi}$ ), and at the Reynolds number of that run, divided by the experimental value of  $(Re_\theta/M_e)_{tr}$  at the same Reynolds number but at the reference (smooth) surface finish ( $k_0$ ), and at the reference surface temperature ( $0.42T_i$ ). Recall that reference, smooth-body transition data were not obtained for the Tunnel F flows. To obtain approximate values of  $\xi$ , the roughness-influenced transition location determined for a given flow condition was divided by a reference value obtained using the smooth-body correlation of NASA-JSC for the same flow condition. As a result there is greater uncertainty in the values of  $\xi$  for the Tunnel F tests. Nevertheless, the correlation between  $\xi$  and  $Re_{k,x=0.1L}$  is approximately the same both for the misaligned-tile models and for the grit-roughened model.

Surface roughness had no measurable effect on the transition location for  $Re_{k,x=0.1L} < 30$ . This is the incipient value of  $Re_{k,x=0.1L}$ , since it is the "point" at which  $\xi$  just decreases below unity. The relative transition parameter decreases slowly as  $Re_{k,x=0.1L}$  increases, until  $Re_{k,x=0.1L}$  reaches a value of 110, which is the critical value. Above this critical value, the relative transition parameter decreases rapidly (i.e., transition moves rapidly upstream toward the nose) until  $Re_{k,x=0.1L}$  reaches a value of 180. Since the distributed

roughness elements now serve as effective tripping devices, 180 is the effective value of  $Re_{k,x=0.1L}$ .

These values for the incipient, the critical, and the effective values of  $Re_{k,x=0.1L}$  are graphically illustrated by the words written in Fig. 8 at the intersections of the linear segments representing approximate fairings of the data.

#### Application to Flight Conditions

To use correlations such as presented in Fig. 8 to predict the effect of surface roughness on boundary-layer transition for the Orbiter during entry,  $Re_k$  must be calculated for flight conditions. The flowfield solutions from Ref. 20 were used to provide distributions of  $Re_y$  across the boundary layer for selected times during the design trajectory, which is designated as 14414.1 in Ref. 12. These distributions of  $Re_y$  at  $x=0.1L$  in the windward pitch plane are presented in Fig. 9. Because  $Re_k$  is relatively insensitive to  $x/L$  at flight conditions, the  $Re_y$  distribution was obtained at one station only, i.e., at  $x=0.1L$ .

The effect of a given misalignment ( $k$ ) on the transition location can be assessed by entering Fig. 9 with the value of  $y$  equal to the  $k$  of interest and determining the corresponding value of  $Re_k$  for a particular time. Once  $Re_k$  is known, the relative change in the smooth-body transition parameter can be determined using Fig. 8 (or an alternative correlation). Knowing the distribution and history of the smooth-body transition parameter and of  $\xi$  gives the value of  $x_{tr}/L$  for the roughened surface for the selected time and roughness. This process was carried out using several values of  $k$  for seven times of the design trajectory. The results showing the effects of roughness on the transition history for the Orbiter pitch plane are presented in Fig. 10. These results can be used to estimate how much earlier in the flight transition would occur at a given station for a given roughness or how much further

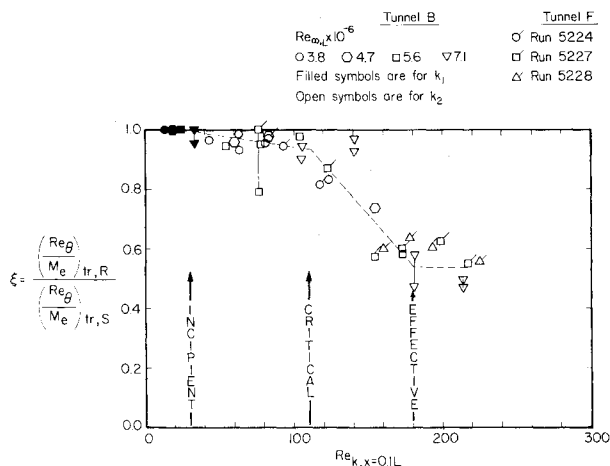


Fig. 8 The relative transition location as a function of  $Re_{k,x=0.1L}$ .

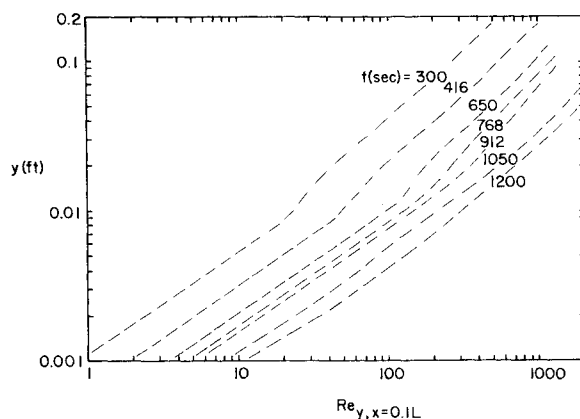


Fig. 9 The  $Re_y$  distribution at  $x = 0.1L$  in the pitch plane.

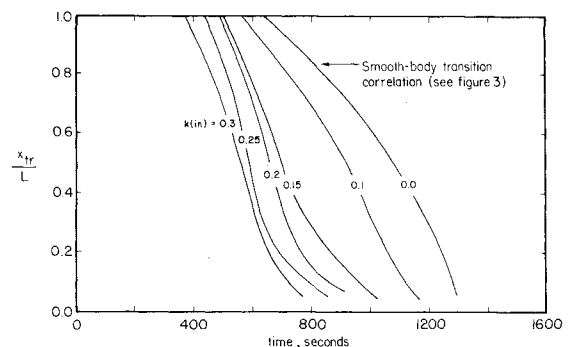


Fig. 10 The predicted effect of a given vertical tile misalignment on the pitch-plane transition location during entry for the 14414.1 trajectory.

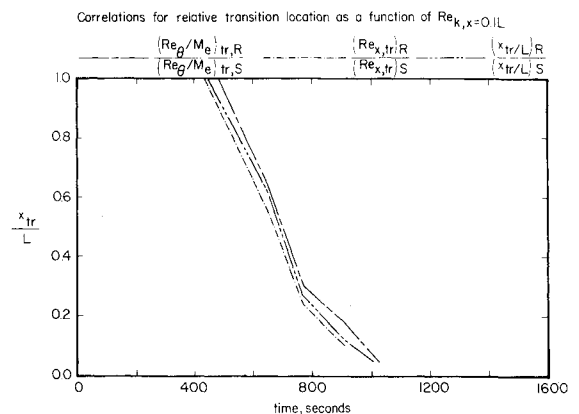


Fig. 11 The effect of selected correlations on the transition-location history for  $k = 0.15$  in. for the 1444.14 trajectory.

upstream transition would occur at a particular time in the trajectory if the tiles were thus misaligned.

The forward movement of transition due to the combined effects of surface roughness and wall cooling as determined using wind-tunnel measurements was correlated using the parameter  $\xi$  in this paper. Other parameters could have been used. The relative transition locations for the same data base were presented in Ref. 22 in terms of the parameter  $\xi_2$ , where

$$\xi_2 = \frac{(x_{tr}/L)k_i T_{wi} Re_{\infty, L}}{(x_{tr}/L)k_0 0.42 T_i Re_{\infty, L}} \quad (3)$$

To indicate the extent to which the transition location can be affected by which correlation is used, different correlations have been used to determine the history of the transition location for the plane of symmetry for the design trajectory (14414.1) if  $k=0.15$  in. The effect of the correlation used on the transition-location history is indicated in Fig. 11. Whether the relative (i.e., rough/smooth transition location) is correlated in terms of  $(Re_\theta/M_e)_{tr}$  as given by Eq. (2), or in terms of  $(x_{tr}/L)$  as given by Eq. (3), or in terms of  $(Re_{x, tr})$  does not seriously affect the transition location histories.

### Concluding Remarks

Theoretical flowfield parameters and heat-transfer distributions were used to analyze and correlate experimental heat-transfer and boundary-layer transition data obtained using a 0.0175-scale model of the Space Shuttle Orbiter. The windward surface was roughened either by simulated tile misalignment or by grit roughness. Data were obtained for Mach numbers from 8 to 12 over a Reynolds number range  $(1.8-17.6) \times 10^6$ , with surface temperatures from 0.114 to  $0.435 T_i$ . For the geometries and for the flow conditions of the present wind tunnel test programs, the following conclusions are made.

1) Tile misalignment did not significantly affect the heat-transfer rates in regions where the boundary layer was either laminar or turbulent. This does not exclude the possibility of locally high heating to very small regions (such as tile corners) which could not be measured.

2) The effect of a given height roughness was essentially the same for the two types of distributed roughness considered, i.e., simulated tile misalignment and grit roughness.

3) Using a roughness Reynolds number  $(Re_k)$  to correlate the upstream movement of the transition location due to surface roughness, one can identify the incipient, the critical, and the effective values of this parameter. The respective values depend on the position at which  $Re_k$  is evaluated. Approximate values for the windward pitch plane of the Shuttle Orbiter are as follows: If  $Re_k$  is evaluated at  $x=0.1L$ , the incipient value is 30, the critical value is 110, and the effective value is 180.

### Acknowledgments

The analysis presented in this paper was sponsored by the NASA Johnson Space Center through Contract NAS 9-13860. The authors would like to express their appreciation to Liz Rich and Janet Brooks for helping prepare the manuscript.

### References

- <sup>1</sup>Dryden, H.L., "Review of Published Data on the Effect of Roughness on Transition from Laminar to Turbulent Flow," *Journal of the Aeronautical Sciences*, Vol. 20, July 1953, pp. 477-482.
- <sup>2</sup>Klebanoff, P.S., Schubauer, G.B., and Tidstrom, K.D., "Measurements of the Effect of Two-Dimensional and Three-Dimensional Roughness Elements on Boundary-Layer Transition," *Journal of the Aeronautical Sciences*, Vol. 22, Nov. 1955, pp. 803-804.
- <sup>3</sup>van Driest, E.R. and Blumer, C.B., "Boundary-Layer Transition at Supersonic Speeds—Three-Dimensional Roughness Effects (Spheres)," *Journal of the Aerospace Sciences*, Vol. 29, Aug. 1962, pp. 909-916.
- <sup>4</sup>Smith, A.M.O. and Clutter, D.W., "The Smallest Height of Roughness Capable of Affecting Boundary-Layer Transition," *Journal of the Aerospace Sciences*, Vol. 26, April 1959, pp. 229-245, 256.
- <sup>5</sup>Braslow, A.L., "A Review of Factors Affecting Boundary-Layer Transition," April 1966, NASA, TND-3384.
- <sup>6</sup>McCauley, W.D., Saydah, A.R., and Bueche, J.F., "Effect of Spherical Roughness on Hypersonic Boundary-Layer Transition," *AIAA Journal*, Vol. 4, Dec. 1966, pp. 2142-2148.
- <sup>7</sup>Braslow, A.L., "Review of the Effect of Distributed Surface Roughness on Boundary-Layer Transition," AGARD Report 254, North Atlantic Treaty Organization, April 1960.
- <sup>8</sup>Anderson, A.D., "Passive Nosedip Technology (PANT) Program, Interim Report, Vol. X, Appendix A: Boundary Layer Transition on Nosedips with Rough Surfaces," SAMS0-TR-74-86, Aerotherm Division/Acurex Corporation, Jan. 1975.
- <sup>9</sup>Reda, D.C., "Correlation of Nosedip Boundary Layer Transition Data Measured in Ballistics-Range Experiments," SAND 79-0649, Sandia Laboratories, Albuquerque, N. Mex., Nov. 1979.
- <sup>10</sup>Bertin, J.J., Idar, E.S. III, and Goodrich, W.D., "Effect of Surface Cooling and Roughness on Transition for the Shuttle Orbiter," *Journal of Spacecraft and Rockets*, Vol. 15, March-April 1978, pp. 113-119.
- <sup>11</sup>Bertin, J.J., Neal, D.R., and Stalmach, D.D., "The Effect of the Transport Property Models on the Shuttle Boundary Layer," Aerospace Engineering Report 78002, The University of Texas at Austin, June 1978.
- <sup>12</sup>"Space Shuttle Orbiter Entry Aerodynamic Heating Data Book," SD73-SH-0184C, Rockwell International Space Division, Downey, Calif., Oct. 1978.
- <sup>13</sup>Martindale, W.R. and Trimmer, L.L., "Test Results from the NASA/Rockwell International Space Shuttle Test (OH4A) Conducted in the AEDC-VKF Tunnel B," AEDC-DR-74-39, AEDC, May 1974.
- <sup>14</sup>Siler, L.G. and Martindale, W.R., "Test Results from the NASA Space Shuttle Orbiter Heating Test (MH-2) Conducted in the AEDC-VKF Tunnel B," AEDC-DR-75-103, AEDC, Oct. 1975.
- <sup>15</sup>Wannenwetsch, W.D. and Martindale, W.R., "Roughness and Wall Temperature Effects on Boundary-Layer Transition on a 0.0175 Scale Space Shuttle Orbiter Model Tested at Mach Number 8," AEDC-TR-77-19, AEDC, April 1977.
- <sup>16</sup>Boudreau, A.H., "Test Results from the NASA/RI Shuttle Heating Test OH-11 in the AEDC-VKF Tunnel F," AEDC-DR-74-16, AEDC, Feb. 1974.
- <sup>17</sup>Siler, L.G., "Test Results from the NASA Space Shuttle Orbiter Heating Test (MH-1) Conducted in the AEDC-VKF Tunnel F," AEDC-DR-76-13, AEDC, March 1976.
- <sup>18</sup>Fay, J.A. and Riddell, F.R., "Theory of Stagnation Point Heat Transfer in Dissociated Air," *Journal of the Aeronautical Sciences*, Vol. 25, Feb. 1958, pp. 73-85 and 121.
- <sup>19</sup>Bertin, J.J. and Cline, D.D., "Variable-Grid-Size Transformation for Solving Nonsimilar Laminar and Turbulent Boundary-Layers," *Proceedings of the 1980 Heat Transfer and Fluid Mechanics Institute*, Stanford University Press, Stanford, Calif., 1980, pp. 135-166.
- <sup>20</sup>Goodrich, W.D., Li, C.P., Houston, C.K., Chiu, P., and Olmedo, L., "Numerical Computations of Orbiter Flow Fields and Laminar Heating Rates," *Journal of Spacecraft and Rockets*, Vol. 14, May 1977, pp. 257-264.
- <sup>21</sup>Bertin, J.J., Idar, E.S. III, and Galanski, S.R., "Effect of Surface Cooling and Roughness on the Heating (Including Transition) to the Windward Plane-of-Symmetry of the Shuttle Orbiter," Aerospace Engineering Report 77002, The University of Texas at Austin, April 1977.
- <sup>22</sup>Bertin, J.J., Hayden, T.E., and Goodrich, W.D., "Comparison of Correlations of Shuttle Boundary-Layer Transition Due to Distributed Roughness," AIAA Paper 81-0417, Jan. 1981.